Journal of Optoelectronics and Advanced Materials Vol. 4, No. 2, June 2002, p. 337 - 340

STRUCTURE AND MAGNETIC PROPERTIES OF Ni-Zn-Cu FERRITES SINTERED AT DIFFERENT TEMPERATURES

O. F. Caltun, L. Spinu[a], Al. Stancu

"Al. I. Cuza" University, Faculty of Physics, 11 Blvd. Copou, 6600 Iasi, Romania
[a]AMRI, University of New Orleans, LA 70148, USA.

Microstructure and magnetic properties of Ni-Zn ferrite are highly sensitive to the preparation methodology, sintering conditions and to the amount of constituent metal oxides, impurities or doping levels. This paper focuses its discussion on the dependence of permeability spectra of the hysteresis loop and magnetic properties on the frequency for samples of Ni-Zn-Cu ferrite sintered at different temperatures. The experimental and calculated complex permeability curves are compared. The values of the parameter β representing the damping factor of the domain wall motion obtained by fitting the permeability spectra are compared with the parameter obtained in the Jiles - Atherton model.

(Received February 27, 2002; accepted May 15, 2002)

Keywords: Magnetic properties of ferrites, Magnetic permeability, Frequency dependence, Jiles-Atherton model

1. Introduction

In order to develop multilayer chip inductor the Ni-Zn-Cu ferrite was intensively studied in the last ten years [1-3]. The interfacial reaction, between the ferrite and the Ag electrode, can be suppressed by co-firing at low temperature the ensemble. The ferrite sintered at different temperatures presents different microstructure and consequently different magnetic properties. The complex permeability spectra and the hysteresis loop are discussed from the point of view of the spin and domain wall contributions in magnetization process. The experimental and theoretical results are compared using Nakamura [4] and Jiles-Atherton [5] models for complex permeability and hysteresis loop, respectively.

2. Experimental results

A conventional ceramic technique was used to obtain ferrite with chemical formula: $Ni_{0.8-x}Cu_xZn_yFe_2O_4$, with x = 0 and y = 0.2. The sample without copper was denoted by N0 and was sintered at maximum temperature 1300^0C. Five categories of sample added with copper oxide (x = 0.15 and y = 0.2) were obtained by sintering the cores at different temperatures. The samples denoted by $N_{1...5}$ were sintered at more elevated temperatures, 1100^oC, 1150^oC, 1200^oC, 1250^oC and 1300^oC, respectively [6].

The microstructure was studied using SEM technique (JEOL 5410 Microscope). The microstructure of the samples depends on the sintering temperature and copper doping as is illustrated in Fig. 1. By adding copper in the sintering process one observes that same average grain size is obtained at lower temperature. Increasing the sintering temperature the sintering density increases and the particles' size are more uniform. The presence of copper oxide in the sintering processes improves the increase of the average grain size simultaneously with porosity decrease. The grain size and the porosity play an important role in magnetisation processes and determine the magnetic properties of

the samples. The ferrite grain size has an important influence on the domain wall contributions in the magnetisation processes at low frequency. The porosity influences the domain wall susceptibility.

The frequency dependence of the complex initial permeability at room temperature has been measured by using the conventional technique based on the determination of the complex impedance of a circuit loaded with a toroid shaped sample (Hewlett Packard 4194A Impedance Analyser). Fig. 2 shows the real and imaginary permeability spectra, respectively for all the samples. As sintering temperature increases, the natural resonance frequency, shifted toward low frequency from 3 MHz to 0.5 MHz. This result confirms that by increasing the sintering temperature over 1200°C, large ferrite particles are obtained and the domain wall motion plays an important role in magnetisation process at low frequency.

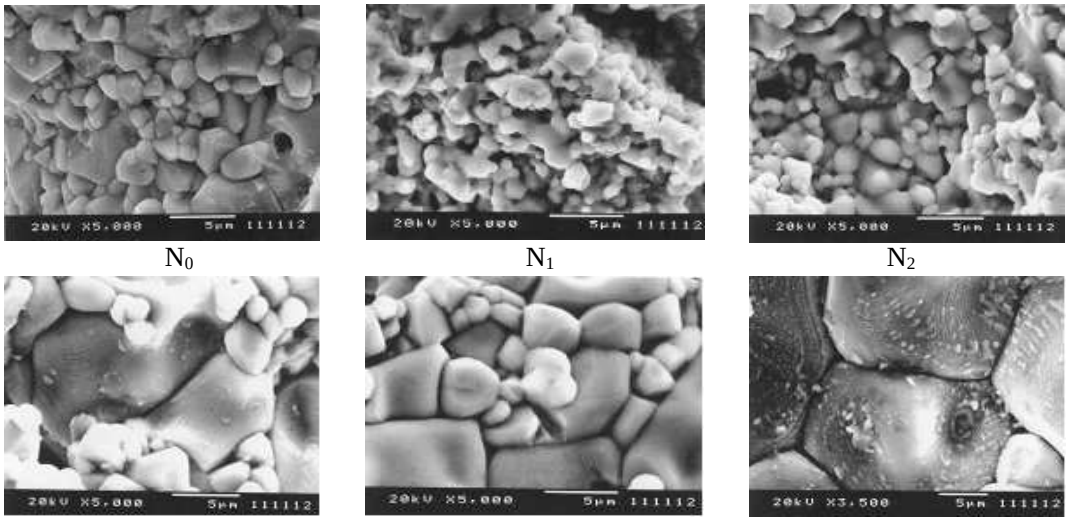

N_0 N_1 N_2

N_3 N_4 N_5

Fig. 1. The microstructure of the samples.

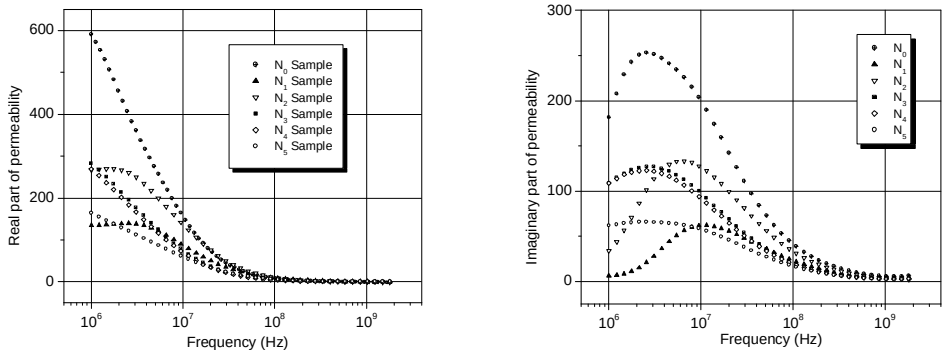

(a) (b)

Fig. 2. The real part (a) and the imaginary part (b) of the permeability.

The complex permeability of sintered ferrite is related to two different magnetising mechanisms: the spin rotational magnetisation and the domain wall motion. In order to make some detailed discussions, Nakamura [4] decomposed the permeability spectra of the sintered ferrite into the spin rotational component, $\chi_{sp}(\omega)$, and the domain wall component, $\chi_{dw}(\omega)$. The spin rotational component is of relaxation type and its dispersion is inversely proportional to the frequency. The domain wall component is of resonance type and depends on the square of frequency. There are few parameters in the model: K_{sp} the static spin susceptibility, ω_{sp} the spin resonance frequency, K_{dw} the static susceptibility of the domain wall motion, ω_{dw} the domain wall motion frequency and β the damping factor of the domain wall motion. The parameters can by determined by numerical

fitting of the complex permeability spectra. In Fig. 3 are presented the experimental and calculated curves for sample N_2. A very good agreement was observed for the real parts of the permeability spectra for all samples. Table 1 summarises the parameters for all the samples. One observes that parameter β, representing the damping factor depends on grains size and porosity. Sample N2 presents the highest value.

In order to confirm that the domain wall motion plays an important role at low frequency in the magnetisation processes the dependence on the frequency of the hysteresis loop was studied. Hysteresis loops for all the samples at different frequencies were obtained using a self made hysteresisgraph [7]. Sinusoidal waveforms with the frequency ranging between 20Hz and 20MHz were used. The maximum value of the magnetic field strength was 80A/m in the low frequency region (20…20kHz). The maximum value of the magnetic field strength in the high frequency region (20kHz…20MHz) was 8A/m. Fig. 4 features the hysteresis loops obtained at 20kHz for all the samples. The shape of the hysteresis loop depends on the microstructure of the sample. The saturation and remanence magnetic flux densities decrease by increasing the excitation frequency. The comparison between the behaviour of the sample N_0, without copper and sintered at 1300ºC, with the sample N_5, added with copper and sintered at the same temperature, reveals that the addition of copper oxide contributes to the decrease of coercive magnetic field strength. Increasing the sintering temperature the squarness of hysteresis loops becomes smaller.

Table 1. The characteristic parameters for N_i samples.

Samples	K_{sp}	K_{dw}	ω_{sp} (MHz)	ω_{dw} (MHz)	β (kHz)
N_0	225	438	13	0.71	2.3
N_1	119	21	11.3	8.17	9.6
N_2	67	210	33.5	2.1	470
N_3	210	94	2.5	1.11	88
N_4	1463	4249	15.5	1.53	170
N_5	1585	4325	14.4	2.31	274

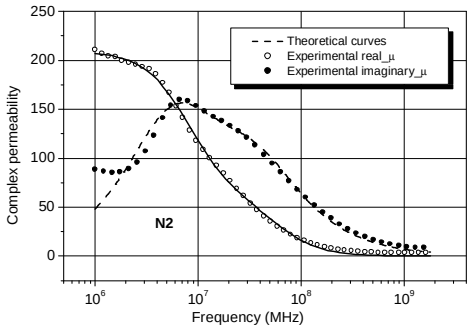

Fig. 3. The experimental and calculated complex permeability for the sample N_2.

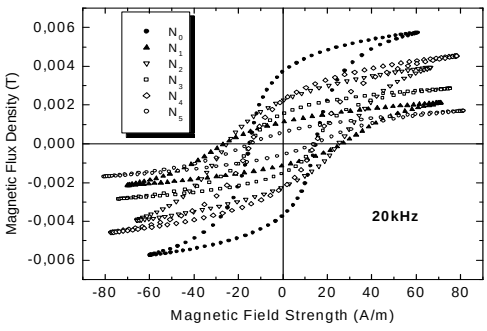

Fig. 4. The experimental and calculated hysteresis loops in J-A model for all the samples at 20kHz.

In the Jiles-Atherton model of hysteresis the magnetic susceptibility is a function of the magnetisation M and the applied magnetic field H [5, 8]. Few parameters are used in the model: a is the form factor for the anhysteretic curve, c is approximately the ratio of the initial susceptibility on the first magnetisation curve to the initial anhysteretic differential susceptibility, α is a parameter representing the coupling between domains, k is the pinning constant (it gives a measure of the width of the hysteresis loop) and M_s is the saturation magnetisation. All these parameters can be calculated from experimental values of the coercive field (H_c), remanent magnetisation (M_r), saturation magnetisation (M_s), initial anhysteretic susceptibility (χ_{an}), initial susceptibility measured on the first magnetisation curve (χ_{in}), maximum differential susceptibility (χ_c) and differential susceptibility at

remanence (χ_r) [9]. Table 2 summarises the model parameters determined for all the samples at 20 kHz excitation frequency.

The identification method has been performed for all the samples. A few facts are obvious from the above table. The saturation magnetisation has a maximum value for the sample without copper oxide. By adding copper oxide the saturation magnetisation decreases. The parameter α, representing the coupling between domains, has a minimum value for sample N_2 characterised by highest value of the parameter β. The domain wall motion is favoured in the ferrite with small average grain size and low porosity.

Table 2. The model parameters determined for all the samples at 20 kHz excitation frequency.

Sample	M_S (A/m)	k (A/m)	k_0 (A/m)	k_S (A/m)	A (A/m)	S	α
N_0	5300	17	0.12	38	12	1	0.0046
N_1	2290	33	0.70	32	19	1	0.0027
N_2	4000	40	0.06	24	15	1	0.0023
N_3	2550	16	0.05	34	10	1	0.0036
N_4	4150	16	0.06	38	12	1	0.0021
M_5	1550	14	0.04	38	12	1	0.0010

3. Conclusions

The addition of copper oxide changes the sintering temperature for Ni-Zn-Cu ferrite. Samples with more uniform microstructure and lower porosity were obtained at low sintering temperature. Increasing the sintering temperature the average grain size increases. The sample N_0, without copper oxide, is characterised by lowest average grain size, lowest damping factor β and highest coupling parameter α. These remarks demonstrate that the results in Nakamura model for complex permeability spectra analysis could be correlated with the results obtained in Jiles – Atherthon model of hysteresis.

References

[1] T. Nomura, A. Nakano, 6th International Conference on Ferrites, Conference Digest, ICF6, The Japan Society of Powder and Powder Metallurgy, ISBN 4-9900214-1-X, ISSN 0918-5070, Tokyo, Japan, Sept 29- Oct 2, p.1198 (1992).
[2] S. F. Wang, Y. R. Wang, T. C. K. Yang, C. F. Chen, C. A. Lu, C. Y. Huang, J. Magn. Magn. Mater. **220**, 129 (2000).
[3] T. Nakamura, J. Magn. Magn. Mater. **168**, 285 (1997).
[4] T. Nakamura, J. Appl. Phys. **88**, 348 (2000).
[5] P. Andrei, O. F. Caltun, C. Papusoi, A. Stancu, M. Feder, J. Magn. Magn. Mater. **196– 197**, 362 (1999).
[6] O. F. Caltun, L. Spinu, Al. Stancu, L. D Tung, W.L. Zhu, to be published in J. Magn. Magn. Mater. (2002).
[7] A. Stancu, O. Caltun, P. Andrei, J. Phys IV France, C1, Suppl. Mars 1997, p. CI.209.
[8] D. C. Jiles, IEEE Trans. Magn. **29**, 3990 (1993).
[9] P. Andrei, O. Caltun, Al. Stancu, IEEE Trans. Magn. **34**, 231 (1998).